Am J Physiol Lung Cell Mol Physiol 315: L742–L751, 2018.
First published August 9, 2018; doi:10.1152/ajplung.00184.2018.

RESEARCH ARTICLE

Sodium nitrite augments lung *S*-nitrosylation and reverses chronic hypoxic pulmonary hypertension in juvenile rats

Robert P. Jankov,[1,2,3,4] Kathrine L. Daniel,[1] Shira Iny,[1] Crystal Kantores,[4] Julijana Ivanovska,[4] Nadya Ben Fadel,[2] and Amish Jain[5,6]

[1]*Molecular Biomedicine Program, Children's Hospital of Eastern Ontario Research Institute, Ottawa, Ontario, Canada;* [2]*Faculty of Medicine, Department of Pediatrics, University of Ottawa, Ottawa, Ontario, Canada;* [3]*Faculty of Medicine, Department of Cellular and Molecular Medicine, University of Ottawa, Ottawa, Ontario, Canada;* [4]*Translational Medicine Program, Hospital for Sick Children Research Institute, Toronto, Ontario, Canada;* [5]*Department of Physiology, University of Toronto, Toronto, Ontario, Canada; and* [6]*Lunenfeld-Tanenbaum Research Institute, Mount Sinai Hospital, Toronto, Ontario, Canada*

Submitted 19 April 2018; accepted in final form 6 August 2018

Jankov RP, Daniel KL, Iny S, Kantores C, Ivanovska J, Ben Fadel N, Jain A. Sodium nitrite augments lung *S*-nitrosylation and reverses chronic hypoxic pulmonary hypertension in juvenile rats. *Am J Physiol Lung Cell Mol Physiol* 315: L742–L751, 2018. First published August 9, 2018; doi:10.1152/ajplung.00184.2018.—Deficient nitric oxide (NO) signaling plays a critical role in the pathogenesis of chronic neonatal pulmonary hypertension (PHT). Physiological NO signaling is regulated by *S*-nitrosothiols (SNOs), which act both as a reservoir for NO and as a reversible modulator of protein function. We have previously reported that therapy with inhaled NO (iNO) increased peroxynitrite-mediated nitration in the juvenile rat lung, although having minimal reversing effects on vascular remodeling. We hypothesized that sodium nitrite ($NaNO_2$) would be superior to iNO in enhancing lung SNOs, thereby contributing to reversal of chronic hypoxic PHT. Rat pups were exposed to air or hypoxia (13% O_2) from postnatal *days 1* to *21*. Dose-response prevention studies were conducted from *days 1–21* to determine the optimal dose of $NaNO_2$. Animals then received rescue therapy with daily subcutaneous $NaNO_2$ (20 mg/kg), vehicle, or were continuously exposed to iNO (20 ppm) from *days 14–21*. Chronic PHT secondary to hypoxia was both prevented and reversed by treatment with $NaNO_2$. Rescue $NaNO_2$ increased lung NO and SNO contents to a greater extent than iNO, without causing nitration. Seven lung SNO proteins upregulated by treatment with $NaNO_2$ were identified by multiplex tandem mass tag spectrometry, one of which was leukotriene A4 hydrolase (LTA4H). Rescue therapy with a LTA4H inhibitor, SC57461A (10 $mg \cdot kg^{-1} \cdot day^{-1}$ sc), partially reversed chronic hypoxic PHT. We conclude that $NaNO_2$ was superior to iNO in increasing tissue NO and SNO generation and reversing chronic PHT, in part via upregulated SNO-LTA4H.

cofilin; leukotriene; newborn; nitration; nitric oxide

INTRODUCTION

Chronic pulmonary hypertension (PHT), characterized by increased pulmonary vascular resistance (PVR), increased pulmonary arterial pressure, and arterial wall remodeling due to smooth muscle hyperplasia (46) is commonly observed in newborns and infants with bronchopulmonary dysplasia and other developmental lung disorders. Chronic PHT heralds a greatly increased risk of death and severe morbidity, and no therapies yet exist that are proven to modify the disease course (32). Abundant evidence implicates deficient nitric oxide (NO) signaling as central to the pathogenesis of chronic neonatal PHT (12, 13, 26, 50). In addition to endothelial NO synthase (NOS)-derived NO stimulating signaling pathways leading to vascular smooth muscle relaxation, physiological NO signaling is regulated by reversible *S*-nitrosylation of cysteine thiols (47), producing *S*-nitrosothiols (SNOs) (20). *S*-nitrosylation modifies protein structure, alters interactions with binding partners, or leads to changes in subcellular localization and degradation, causing a reversible alteration in protein function (2, 19, 24, 36, 49).

Exogenous (inhaled) NO (iNO) is a commonly utilized NO-based therapy in the neonate. Unfortunately, iNO has not proven effective at reversing or slowing progression of chronic PHT in human infants (5, 11) and has been of variable efficacy in reversing established chronic PHT in neonatal rats (31, 50). A biochemical obstacle to effective NO-based therapy relates to the high potential for NO to be diverted to produce reactive nitrogen species such as peroxynitrite (31); particularly in the lung, which is directly exposed. Reactive nitrogen species cause irreversible oxidation and tyrosine nitration (51), which permanently alters protein function (6, 23, 59) and directly contributes to pulmonary vascular disease in neonatal rats (7, 15, 31, 35).

Nitrite anion (NO_2^-) is now recognized to contribute importantly to local NO bioavailability and to SNO formation by acting as a stable, nonreactive endocrine pool of NO, formed from circulating and tissue-bound NO_2^- reductases (1, 52). Unlike adults, in whom the majority of circulating NO_2^- is derived from dietary nitrate, sources of nutrition in neonates are poor in NO_2^- (33), resulting in lower plasma NO_2^- levels (30) and a likely greater dependence upon NOS to generate NO. Inhaled ethyl (alkyl) nitrite, a volatile gas that acts as a NO_2^- donor, was more effective than iNO in preventing hyperoxic lung injury in neonatal rats (3) and was highly efficacious as an acute pulmonary vasodilator in human neonates (38). These observations support NO_2^--based therapy as a promising strategy. Systemic or inhaled sodium nitrite ($NaNO_2$) is an

Address for reprint requests and other correspondence: R. P. Jankov, Children's Hospital of Eastern Ontario, 401 Smyth Rd., Ottawa, ON, K1H 8L1, Canada (e-mail: rjankov@cheo.on.ca).

alternative NO_2^--based therapy shown to be strongly protective in adult experimental models of chronic PHT (4, 17, 28, 41, 61). However, no previous studies, to our knowledge, have examined effects of $NaNO_2$ on chronic PHT in the neonatal or juvenile animal. We hypothesized that therapy with $NaNO_2$ will be superior to iNO in enhancing NO bioavailability and *S*-nitrosylation, thus allowing for rescue of chronic hypoxic PHT.

Herein, we report that systemically administered $NaNO_2$ both prevented and reversed chronic hypoxic PHT and increased lung NO and SNO contents to a far greater extent than iNO. Furthermore, unlike iNO, $NaNO_2$ did not increase lung nitration. We identified several lung SNO proteins upregulated by $NaNO_2$ therapy, including SNO leukotriene (LT) A4 hydrolase (LTA4H). Rescue effects of $NaNO_2$ were partially replicated by an LTA4H inhibitor, SC57461A, suggesting increased SNO-LTA4H as one mechanism by which $NaNO_2$ reversed chronic PHT.

MATERIALS AND METHODS

Materials. Sodium nitrite ($NaNO_2$; cat. no. S-2252) and SC57461A (cat. no. 3107) were purchased from Sigma-Aldrich (Oakville, Canada) and Tocris Biosciences (Bristol, UK), respectively. *S*-nitrosylated biotin switch (cat. no. 10006518) and nitrate/nitrite detection (cat. no. 780001) kits, peroxynitrite solution (cat. no. 81565), and C18 solid phase extraction cartridges (cat. no. 400020) were from Cayman Chemical (Ann Arbor, MI). Oxygen and NO exposure chambers and automated controllers, OxyCycler models A84XOV and AT2N, were from Biospherix (Parish, NY). NO 400-ppm cylinders (balance N_2) were from Linde Canada (Mississauga, Canada). Iodo-tandem mass tag (TMT) labeling kits (cat. nos. 90100 and 90101), immobilized anti-TMT antibody resin (cat. no. 90076), and TMT elution buffer (cat. no. 90104) were from Thermo Fisher (Waltham, MA). Mass spectrometry grade Trypsin/Lys-C mix (cat. no. V-5072) was from Promega (Madison, WI). Precast Tris-glycine 4–20% gradient gels (mini-PROTEAN TGX Stain-Free), chemiluminescent reagent (Clarity or Clarity Max Western ECL substrate), imaging system (Chemi-Doc Touch), and analysis software (Image Laboratory 6.0) were from Bio-Rad (Mississauga, Canada). Protease inhibitors were from Calbiochem (cat. no. 539131-10-VL, San Diego, CA). Acids, alcohols, organic solvents, paraformaldehyde, Permount, and Superfrost/Plus microscope slides were from Thermo Fisher. Weigert's resorcin-fuchsin stain was from Rowley Biochemical (cat. no. F-370-1, Danvers, MA). Avidin-biotin-peroxidase complex (cat. no. PK-6100) and 3,3-diaminobenzidine staining kits (cat. no. PK-4100) were from Vector Laboratories (Burlingame, CA). An antigen retriever device was from Aptum Biologics Ltd. (Antigen Retriever 2100, Southampton, United Kingdom). IHC-Tek antibody diluent (cat. no. IW-1000) and epitope retrieval solution (cat. no. IW-1100) were from IHC World (Woodstock, MD). Anti-LTA4H (cat. no. NBP-1-95835) was from Novus Biologicals (Littleton, CO). Anti-nitrotyrosine (cat. no. 06-284) was from EMD Millipore (Billerica, MA). Anti-cofilin-1 (cat. no. 5175) and goat anti-rabbit IgG-peroxidase (cat. no. 7074) antibodies were from Cell Signaling Technologies (Beverly, MA). Anti-phospho-serine 695 myosin phosphatase target (MYPT)-1 (cat. no. sc-33360) and goat anti-rabbit IgG-biotin (cat. no. sc-2040) secondary antibody were from Santa Cruz Biotechnology (Santa Cruz, CA). Anti-pan-MYPT-1 was from BD Biosciences (cat. no. 612614; Mississauga, Canada). Colorimetric competitive ELISA kits for biotin (cat. no. K811) and 3-nitrotyrosine (cat. no. K-4158) were from BioVision (Milpitas, CA). ELISA kits for LTB4 (cat. no. ADI-900-068) were from Enzo Life Sciences (Farmingdale, NY). Unless specified, all other chemicals and reagents were from Sigma-Aldrich.

In vivo experiments. All procedures involving animals were approved by the Animal Care Committee at the University of Ottawa and conformed to the guidelines of the Canadian Council on Animal Care. A total of 36 timed-pregnant Sprague-Dawley rats were purchased from Taconic Farms (Germantown, NY). Experiments were conducted in multiples of four litters (2 litters in hypoxia and 2 litters in normoxia, one vehicle-treated, and one drug-treated). Except for samples used for mass spectrometry ($n = 2$ per group, performed twice), sample size estimates were based on previous work and set a priori [$n = 8$ for cardiac end points (pulmonary hemodynamics and Fulton index) and $n = 6$ for all other end points] incorporating animals from two to three litters per experimental group with equalized sex distribution. Analysis of all end points was conducted in a blinded fashion. Commencing on the day after birth [considered *postnatal day* (*PND*) *1*], litters of Sprague-Dawley rat pups were chronically exposed to normobaric hypoxia (13% O_2) or normoxia (21% O_2) until *PND 21*. Automated controllers (Biospherix) maintained O_2 concentrations to within 0.1% of set point. The room in which chambers were housed had 12-h light/dark cycles. Chamber temperature was maintained at 25 ± 1°C, humidity at 50 ± 10%, and food and water were available ad libitum. Rat pups received daily subcutaneous $NaNO_2$ (5, 10, 20, or 50 mg/kg in 0.9% saline vehicle; 5 μl per g body wt) or vehicle alone from *PNDs 1–21* to determine the dose of $NaNO_2$ that maximally prevented chronic PHT without significantly (>5%) increasing blood methemoglobin (MetHb). For rescue treatment studies, rats received daily subcutaneous $NaNO_2$ (20 mg/kg), which was determined to be the dose that best met the above criteria, or SC57461A (LTA4H inhibitor) at a dose (10 mg·kg^{-1}·day^{-1} sc) previously reported by our group to be effective in neonatal rats (16) or vehicle (0.9% saline or 20% DMSO in PBS, respectively) from *PND 14* to *PND 21*. Separate animals were exposed to chronic hypoxia with or without iNO 20 ppm. Effects of rescue treatment reflect "reversal" of chronic PHT (rather than limiting further progression) as PHT markers have previously been determined in this model to remain stable between *PNDs 14* and *21* (54). Each litter was maintained at $n = 12$ pups throughout the exposure period to control for nutritional effects. At the end of the exposure/treatment period, pups were either killed by pentobarbital overdose or were exsanguinated after inhalational or ketamine-induced anesthesia.

Two-dimensional echocardiography and pulsed wave Doppler ultrasound. Two-dimensional echocardiography and pulsed wave Doppler ultrasound was performed as a noninvasive method to assess pulmonary hemodynamics as previously described (15), using a Philips Affiniti 50 cardiac ultrasound system with a small high frequency linear probe (L15-7io, Philips Healthcare, Richmond Hill, Ontario, Canada). The right ventricular ejection time (RVET) and pulmonary arterial acceleration time (PAAT) were measured using the pulmonary Doppler profile obtained from the parasternal short axis; RVET is the time from onset of systolic flow to completion of systolic flow and PAAT is from onset to peak pulmonary outflow velocity. A previously validated (15) index of PVR was calculated using the average ratio of RVET/PAAT from three systolic traces.

Blood MetHb. At the end of each treatment period, pups were anesthetized as described above and the jugular vein isolated and severed. Blood was collected in a capillary tube and immediately analyzed using an ABL80 FLEX CO-OX blood gas analyzer (Radiometer America, Brea, CA).

Right ventricular hypertrophy. Measurement of right ventricular hypertrophy (RVH) using the Fulton index (right ventricle/left ventricle + septum) is a well-established marker of PHT. The heart and lungs were separated, and the atria were removed inferior to the atrio-ventricular valves. The right ventricle was separated from the left ventricle and septum, freeze-dried, and weighed separately.

Histological studies. Three males and three females (one from each of three litters per group) were euthanized by sodium pentobarbital overdose. Following the opening of the thoracic cavity and tracheal cannulation, the pulmonary veins were divided. The pulmonary cir-

culation was flushed with PBS and heparin (1 U/ml) to clear the lungs of blood, following which the lungs were perfusion-fixed with paraformaldehyde while air inflated at constant pressure (20 cm of H_2O). Following dehydration and clearance in xylene, whole left lungs were embedded in paraffin, cut into 5-μm sections, mounted, air-dried, and baked overnight at 43°C. For elastin staining, sections were dewaxed by immersion in xylene, rehydrated in ethanol, rinsed in several washes of distilled water, and then left overnight in Weigert's resorcin-fuchsin (Hart's elastin) stain. Slides were then washed with distilled water and counterstained with 0.25% (vol/vol) tartrazine in acetic acid followed by dehydration and mounting. Percentage medial wall area (%MWA) was measured on elastin-stained sections as a marker of pulmonary vascular remodeling. Pulmonary arteries (20–100-μm external diameter) were identified by the presence of an inner and outer elastic lamina and proximity to respiratory bronchioles. A minimum of 40 arteries per animal from 4 unique left lung sections were digitally captured and analyzed. Obliquely sectioned vessels where there was a greater than three times difference in perpendicular dimensions were excluded. As previously described (34), using the "Quick Selection" tool (Adobe Photoshop CS5, Adobe Systems Inc., San Jose, CA) the area of the inner lumen and the whole vessel was outlined and pixel count determined. The following formula was used to determine the percent medial wall area: [(whole vessel area−inner luminal area)/whole vessel area] × 100. For 3-nitrotyrosine immunostaining, slides were incubated with anti-nitrotyrosine (1:100) in antibody diluent overnight at 4°C, followed by biotin-conjugated secondary antibody (1:1,000) for 2 h at room temperature, then washed, dehydrated, counterstained with hematoxylin, and mounted.

Measurement of NO oxidation products. Nitrate/nitrite oxidation (NOx) was measured in lung tissue homogenized in PBS and deproteinated by ultrafiltration (Amicon Ultra, EMD Millipore, Burlington, MA). Nitrate in deproteinated samples was enzymatically converted to nitrite (Cayman nitrite/nitrate detection kit) and quantified, along with nitrite standards, using a Sievers 280i NO analyzer (Zysense, Weddington, NC), according to the supplier's instructions. Values were normalized to wet tissue weight.

Quantification and identification of SNO proteins. SNO protein modifications, because of their labile nature, can be difficult to study employing traditional methods used for detecting phosphorylated proteins. For this reason, several "switch" assays have been developed to label SNO-modified cysteines with stable markers (18, 39). Total SNOs were quantified in lung tissue homogenates using a biotin switch assay and competitive biotin ELISA, both according to the manufacturer's instructions. Specific SNO proteins were identified from lung tissue homogenates (two normoxia-exposed vehicle-treated, two hypoxia-exposed vehicle-treated, and two hypoxia-exposed $NaNO_2$-treated) labeled with sixplex-TMT and affinity column purified according to the manufacturer's instructions. Samples were quantified by multiplex liquid chromatography/TMT spectrometry (TMT-LC/MS/MS; Q Exactive Hybrid Quadrupole-Orbitrap Mass Spectrometer, ThermoFisher Scientific) by the SPARC BioCentre (Hospital for Sick Children, Toronto), following previously reported methods (39). Reporter ions observed in the M2 mass spectrum (126–131), generated from higher-energy collisional dissociation fragmentation, were used for relative quantification between samples. Mass spectrometry data were searched using PEAKS software (58) version 8.0 (Bioinformatics Solutions, Waterloo, Canada) and the reporter ions quantified using Proteome Discoverer software (version 2.2; ThermoFisher Scientific). Seven SNO proteins were identified (Table 1) where content was altered (significance score > 2) by $NaNO_2$ treatment with results that were consistent between two separate sets of samples and TMT-LC/MS/MS runs. Two of the seven candidates (LTA4H and cofilin-1) were confirmed by Western blot, despite LC/MS/MS identifying one unique peptide with relatively low sequence coverage (9 and 7%, respectively; Table 1).

Western blot analyses. Lung lysates from three males and three females per group (representing 3 litters) were TMT-labeled according to the manufacturer's instructions, purified by agarose bead immunoprecipitation, and matched with unlabelled, unpurified lysates both of which were separated under reducing conditions by SDS-PAGE. Following electrophoresis, proteins were transferred to PVDF membranes. All membranes were blocked with 5% skim milk for 1 h at room temperature, followed by incubation with primary antibody overnight at 4°C. Blots were then washed with Tris-buffered saline-Tween 20 and placed in secondary antibody for 1 h at room temperature. Dilutions of primary antisera were 1:10,000 for LTA4H (70 kDa) and secondary antiserum and 1:1,000 for Cofilin-1 (19 kDa), phospho-serine 695 and pan-MYPT-1 (80 kDa). Bands were quantified by digital densitometry of nonsaturated images with background density removed. Bands were normalized to corresponding pan-protein content, each corrected for total protein/lane quantified by stain-free protein imaging (Bio-Rad). In preliminary experiments, we confirmed that stain-free protein imaging was equivalent to GAPDH as a marker of protein loading (data not shown). Raw values are expressed as a multiple or fraction of the normoxia-exposed, vehicle-treated group, which was assigned a value of 1.

ELISA. Lung lysates from three males and three females per group (representing 3 litters) were purified and analyzed according to the manufacturer's instructions. Values were normalized to protein content (3-nitrotyrosine) or wet tissue weight (LTB4).

Data presentation and statistical analysis. Data are expressed as means ± SE after any outliers (≥2 SD from mean value) were removed. Analyses were performed using Sigma Plot 13 (Systat software, San Jose, CA). Statistical significance ($P < 0.05$) was determined by *t*-test or one-way ANOVA followed by Tukey post hoc test where significant intergroup differences were found or by Kruskal-Wallis one-way ANOVA for nonparametric data.

Table 1. *Candidate SNO proteins identified by TMT-LC/MS/MS*

Accession No. | Uniprot ID (Protein name)	Unique Peptides, n	Sequence Coverage, %	Known Functions
P30349 | LKHA4 (Leukotriene A_4 hydrolase)	1	9	Epoxy hydrolase catalyzing biosynthesis of proinflammatory leukotriene B_4. Also possesses amino-peptidase activity.
P45592 | COF1 (Cofilin-1)	1	7	Depolymerizes F-actin. Regulates cell morphology and cytoskeletal organization.
B0BMY8 (Histone H3)	2	27	Nucleosomal protein.
Q03348 | PTPA (Serine/threonine-protein phosphatase 2A activator)	1	9	Regulation of apoptosis.
Q63357 | MYO1D (Unconventional Myosin-Id)	2	2	Cytoskeletal protein. Regulation of cell motility.
Q9JLU4 | SHAN3 (SH3 and multiple ankyrin repeat domains protein 3)	1	2	Cytoskeletal protein. Regulation of cell motility.
O35244 | PRDX6 (Peroxiredoxin 6)	1	5	Thiol-specific peroxidase enzyme/antioxidant.

SNO, *S*-nitrosothiols; TMT-LC/MS/MS, multiplex liquid chromatography/TMT spectrometry.

RESULTS

Systemic $NaNO_2$ prevented and reversed chronic hypoxic PHT. Dose response prevention studies are shown in Fig. 1. $NaNO_2$ at doses of 20 and 50 $mg \cdot kg^{-1} \cdot day^{-1}$ prevented chronic PHT as evidenced by significantly ($P < 0.001$) decreased PVR (Fig. 1*A*) and RVH (Fig. 1*B*). Blood MetHb was significantly greater ($P < 0.001$; mean value 7.2%) at 50 mg/kg when compared with 20 mg/kg (mean value 1.75%). Rescue effects of $NaNO_2$ 20 $mg \cdot kg^{-1} \cdot day^{-1}$ are shown in Fig. 2. Rescue $NaNO_2$ normalized PVR (Fig. 2*A*) and almost completely normalized RVH (Fig. 2*B*) and %MWA (Fig. 2*C*). In contrast, and as previously reported (31), iNO had no significant reversing effect on increased RVH (Fulton index 0.481 ± 0.03; $P < 0.001$ vs. $NaNO_2$-treated, $n = 8$ animals per group) or %MWA ($31.1 \pm 2.3\%$; $P < 0.001$ vs. $NaNO_2$-treated, $n = 6$ animals per group) in chronic hypoxia-exposed animals. MetHb values in animals receiving rescue $NaNO_2$ were all <2% (data not shown).

Rescue treatment with $NaNO_2$ increased lung NOx, SNO protein content, and cGMP activity, without causing increased nitration. Lung nitrate/nitrite (NOx) was measured as a marker of total NO content. $NaNO_2$ significantly increased ($P < 0.001$) lung NOx (Fig. 3*A*) and SNO protein (Fig. 3*B*) contents in both normoxia- and hypoxia-exposed animals when compared with animals treated with vehicle- or hypoxia-exposed animals that were treated with iNO. Lung phospho-serine 695/pan-MYPT-1 ratio was used as a marker of cGMP-mediated protein kinase G signaling (PKG), as previously described (42). As shown in Fig. 3*C*, rescue treatment with both $NaNO_2$ and iNO significantly increased lung cGMP-PKG activity in chronic hypoxia-exposed animals. Chronic exposure to hypoxia or treatment with $NaNO_2$ had no effect on total lung 3-nitrotyrosine content (Fig. 3*D*). In contrast, and as previously reported (31), lung 3-nitrotyrosine was greatly increased by rescue treatment with iNO ($P < 0.001$ vs. all other groups; Fig. 3*D*). Representative images of 3-nitrotyrosine immunohistochemistry are shown in Fig. 3*E*.

Rescue treatment with $NaNO_2$ increased lung contents of SNO-LTA4H and SNO-cofilin-1. As shown in Fig. 4, *A* and *B*, SNO-LTA4H and SNO-Cofilin-1 were significantly increased by rescue treatment with $NaNO_2$ in hypoxia-exposed animals. There were no significant differences in pan-LTA4H ($P = 0.125$, by ANOVA; data not shown) or pan-Cofilin-1 ($P = 0.15$, by ANOVA; data not shown) between groups. Increased SNO-LTA4H in $NaNO_2$-treated hypoxia-exposed animals was associated with a nonsignificant ($P = 0.093$) trend toward decreased LTA4H activity, as indicated by lung LTB4 content, when compared with hypoxia-exposed vehicle-treated animals (Fig. 4*D*).

Rescue treatment with SC57461A, a LTA4H inhibitor, partially reversed chronic hypoxic PHT. Treatment with SC57461A partially but significantly ($P < 0.05$), decreased PVR (Fig. 5*A*) RVH (Fig. 5*B*) and %MWA (Fig. 5*C*) in chronic hypoxia-exposed animals. These effects were accompanied by significantly decreased lung LTB4 content (7.2 ± 0.4 pg per lung wet wt in hypoxia-exposed vehicle-treated animals versus 5.4 ± 0.2 in hypoxia-exposed, SC57461A-treated animals, $n = 6$ per group; $P < 0.01$, by *t*-test).

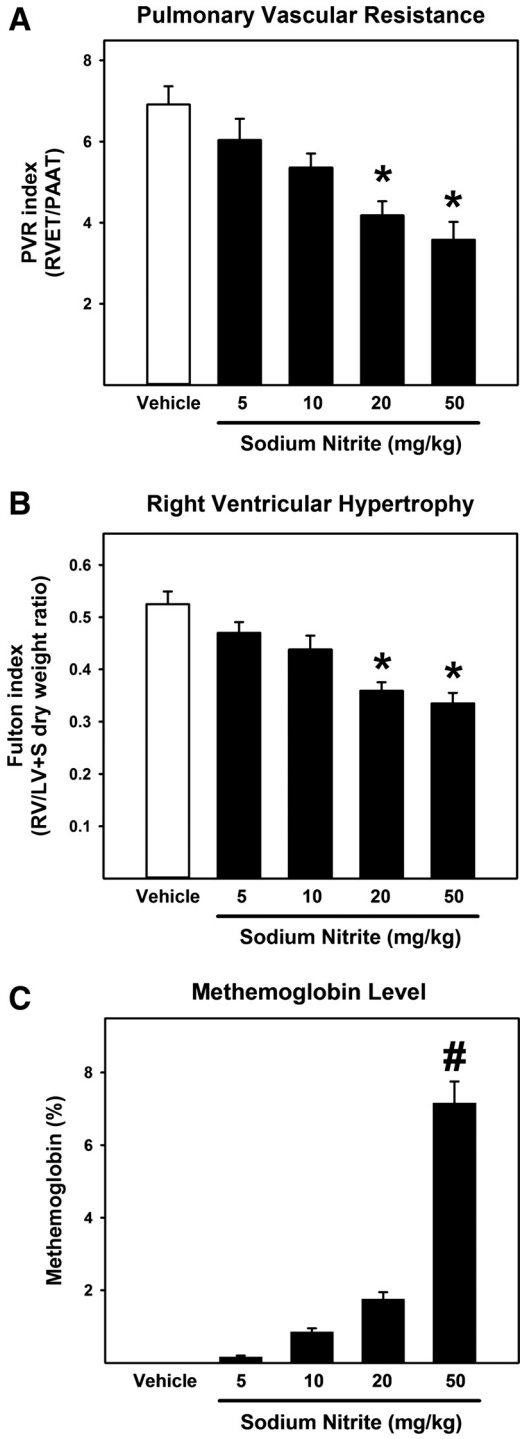

Fig. 1. Dose-response studies. From postnatal *days 1–21*, rat pups were exposed to normobaric hypoxia (13% O_2) or normoxia (21% O_2). Beginning on *day 1*, pups received daily subcutaneous injections of sodium nitrite (5, 10, 20, or 50 mg/kg) or 0.9% saline vehicle. *A*: pulmonary vascular resistance (PVR) index. Ratio of right ventricular ejection time (RVET) to pulmonary arterial acceleration time (PAAT), $n = 8$ animals per group. *B*: right ventricular hypertrophy (RVH) assessed by right ventricle (RV)/left ventricle (LV) + septum (S) weight ratio (Fulton index), $n = 8$ animals per group. *C*: blood percentage methemoglobin levels, $n = 6$ animals per group. Bars represent means ± SE; *$P < 0.001$, by ANOVA, vs. vehicle-treated group. #$P < 0.001$, by ANOVA, vs. all other groups.

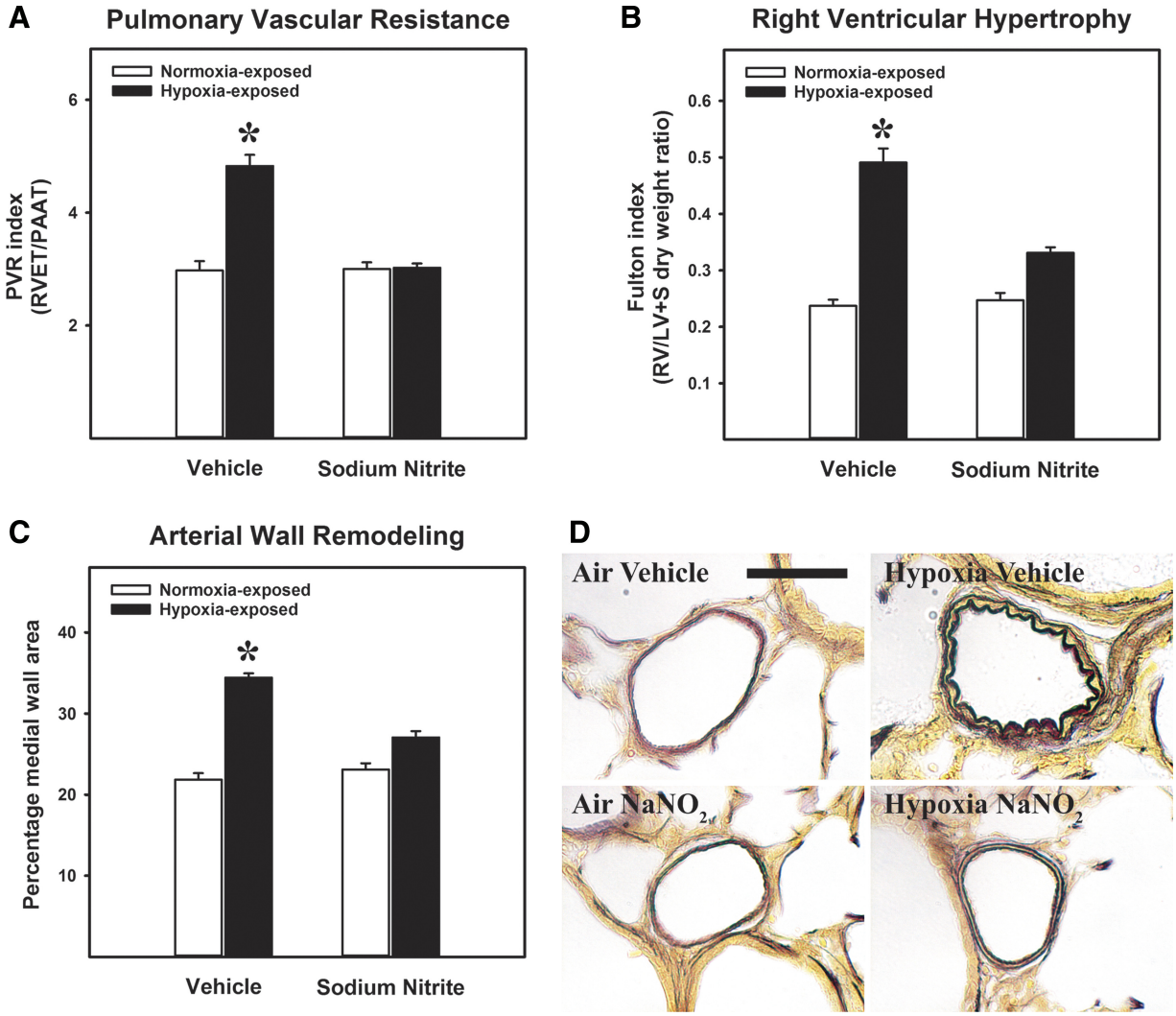

Fig. 2. Rescue sodium nitrite reversed chronic pulmonary hypertension. From *postnatal days 1–21*, rat pups were exposed to normobaric hypoxia (13% O_2; hypoxia) or normoxia (21% O_2). From *days 14–21*, pups received daily subcutaneous injections of sodium nitrite ($NaNO_2$) 20 mg/kg or 0.9% saline vehicle or were continuously exposed to 20 ppm inhaled nitric oxide (iNO). *A*: pulmonary vascular resistance (PVR) index. Ratio of right ventricular ejection time (RVET) to pulmonary arterial acceleration time (PAAT), $n = 8$ animals per group. *B*: right ventricular hypertrophy (RVH) assessed by right ventricle (RV)/left ventricle (LV) + septum (S) weight ratio (Fulton index), $n = 8$ animals per group. *C*: pulmonary arterial medial wall area as a marker of vascular remodeling, $n = 6$ animals per group. Bars represent means ± SE; $^*P < 0.001$, by ANOVA, vs. all other groups. *D*: high-power photomicrographs demonstrating elastin-stained pulmonary arteries. Bar length = 50 μm.

DISCUSSION

We present the first data, to our knowledge, to demonstrate therapeutic efficacy of $NaNO_2$ and superiority to iNO in reversal of chronic PHT in the juvenile animal. $NaNO_2$ has many properties that are favorable for clinical translation, including stability, low cost, and ability to be administered systemically or by inhalation. As confirmed in this study, $NaNO_2$ leads to upregulation of physiological NO signaling [increased SNOs (9, 10, 62)] without an apparent concurrent propensity to cause nitration (14). In humans, an injectable form of $NaNO_2$ is marketed as therapy for cyanide poisoning (25), and nebulized $NaNO_2$ was safe and well tolerated in healthy adults (44) and acutely reduced PVR in pulmonary hypertensive patients with β-thalassemia (56).

In rats chronically exposed to hypoxia from birth, we report that increased PVR, RVH, and pulmonary arterial wall remodeling were almost completely reversed by rescue treatment with systemic $NaNO_2$, in contrast to iNO, which had no significant reversing effect (31). Furthermore, rescue $NaNO_2$ increased lung NOx and total SNO protein contents to a much greater extent than iNO, without causing nitration. In addition to avoidance of nitration, increased bioavailability of NO and enhanced cGMP-PKG signaling, a likely mechanism behind the efficacy of $NaNO_2$ was reversible and specific modification in protein function that arises from *S*-nitrosylation (27). Interestingly, we observed that rescue iNO greatly increased cGMP-PKG activity, which was surprising in light of the lack of reversing effect on markers of chronic PHT. Possible explanations are that enhanced nitration may have negated any benefits of enhanced cGMP signaling and/or that increased *S*-nitrosylation is of greater importance to reversal of pulmonary arterial remodeling in this model.

As there is currently no knowledge on the functional role/s of specific SNO proteins in neonatal cardiopulmonary disease,

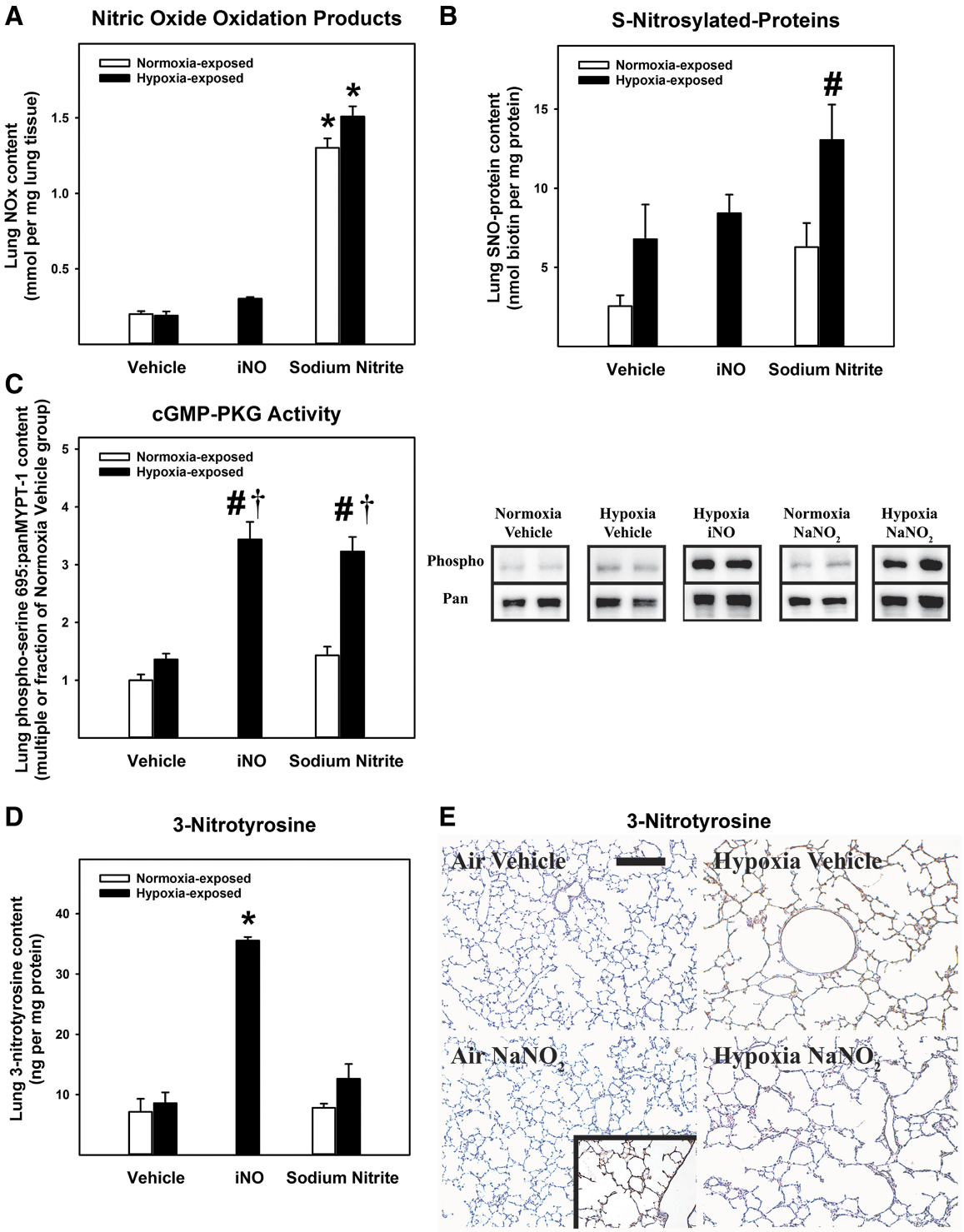

Fig. 3. Rescue sodium nitrite increased lung nitric oxide oxidation (NOx), *S*-nitrosylated (SNO) proteins, and cGMP-PKG activity, without increasing nitration. From *postnatal days 1–21*, rat pups were exposed to normobaric hypoxia (13% O_2; Hypoxia) or normoxia (21% O_2). From *days 14–21*, pups received daily subcutaneous injections of sodium nitrite ($NaNO_2$) 20 mg/kg or 0.9% saline vehicle or were continuously exposed to 20 ppm inhaled nitric oxide (iNO). *A*: lung NOx products as a marker of tissue nitric oxide abundance, $n = 6$ animals/group. *B*: total lung SNO proteins, $n = 6$ animals per group. *C*: Western blot analyses of lung phospho-serine 695/pan-myosin phosphatase target (MYPT)-1 ratio as a marker of cyclic guanosine monophosphate-protein kinase G signaling, $n = 6$ animals per group. Representative immunoblots show two contiguous lanes for each group. *D*: lung 3-nitrotyrosine content, $n = 6$ animals per group. Bars represent means ± SE; *$P < 0.001$, by ANOVA, vs. all other groups. #$P < 0.05$, by ANOVA, vs. normoxia groups. †$P < 0.001$, by ANOVA, vs. vehicle-treated groups. *E*: representative medium-power photomicrographs of lung 3-nitrotyrosine immunoreactivity, as a marker of nitric oxide-derived reactive nitrogen species-mediated nitration. Bar length = 100 μm. *Inset*: positive control section pretreated with 100 mM peroxynitrite.

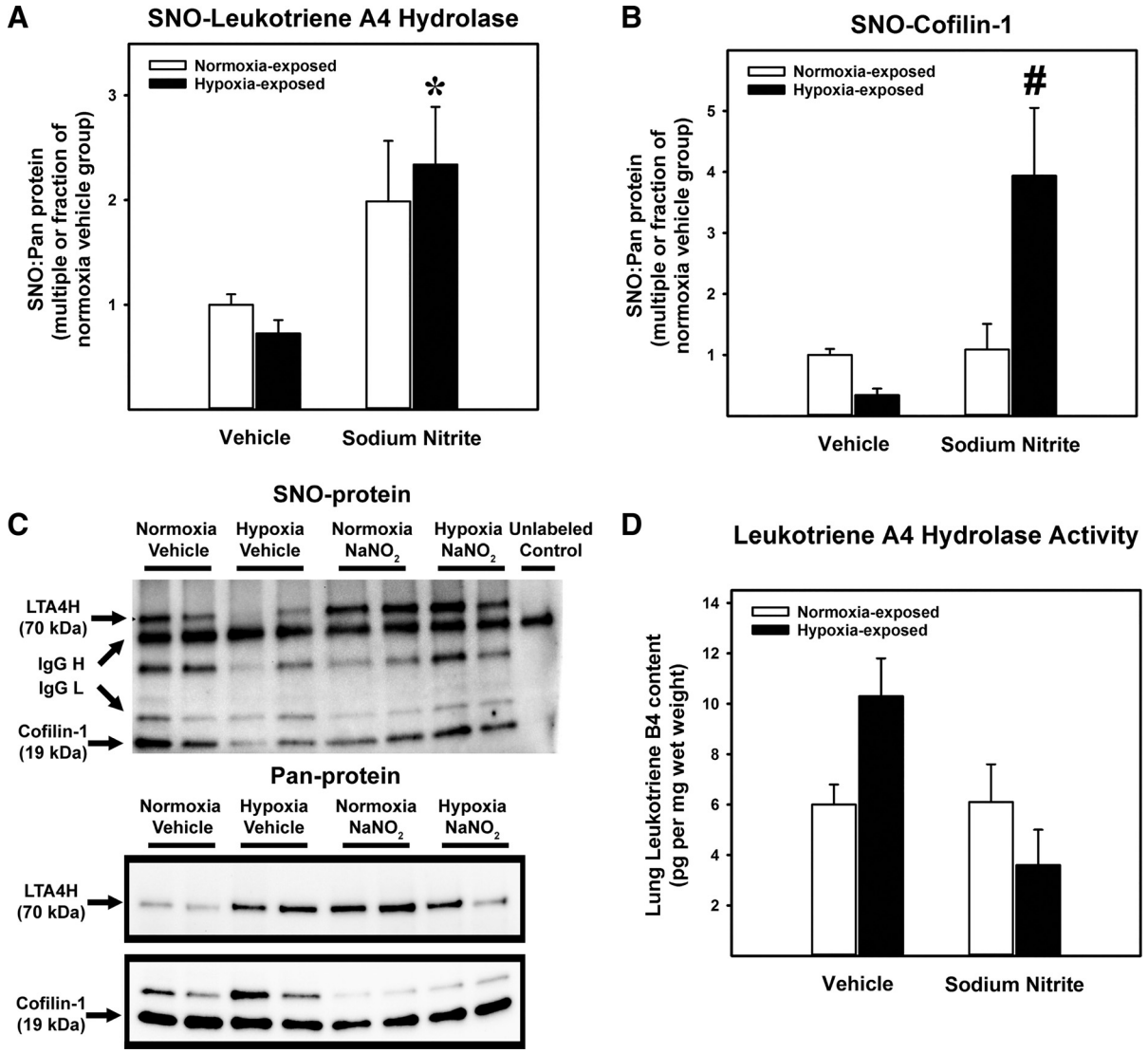

Fig. 4. Rescue treatment with $NaNO_2$ increased lung contents of SNO-leukotrieneA4 hydrolase (LTA4H) and SNO-cofilin-1. From *postnatal days 1–21*, rat pups were exposed to normobaric hypoxia (13% O_2; Hypoxia) or normoxia (21% O_2). From *days 14–21*, pups received daily subcutaneous injections of sodium nitrite ($NaNO_2$) 20 mg/kg or 0.9% saline vehicle. Western blot analyses of lung SNO-LTA4H (*A*) and SNO-cofilin-1 (*B*). Representative immunoblots for SNO and pan-proteins (*C*). Unlabeled control = purified normoxia-exposed, vehicle-treated sample not labeled with TMT. Lung Leukotriene B4, as a marker of LTA4H activity, quantified by ELISA (*D*). Bars represent means ± SE for $n = 5–6$ samples per group. *$P < 0.05$, by Kruskal-Wallis one-way ANOVA, compared with all vehicle-treated groups. #$P < 0.05$, by Kruskal-Wallis one-way ANOVA, compared with all other groups. H, heavy chain; L, light chain; SNO, *S*-nitrosothiols; TMT, tandem mass tag.

we undertook TMT-LC/MS/MS and identified seven lung SNO proteins that were consistently upregulated by treatment with $NaNO_2$. Despite there being relatively low sequence coverage for most peptides identified by LC/MS/MS, changes in two of these proteins, LTA4H and cofilin-1, were able to be confirmed by Western blot analyses. *S*-nitrosylation is the covalent modification of cysteine thiols by addition of a nitrosyl group (by either NO or NO_2^-). As a result, cysteine-rich proteins contribute importantly to physiological NO signaling by acting as a circulating and tissue reservoir for NO (2, 19, 24, 36, 49). In addition, *S*-nitrosylation possesses the essential criteria for a signaling modification (akin to phosphorylation), including a rapid reaction, specificity for particular cysteine residues, and enzymatic removal [by *S*-nitrosoglutathione reductase and the thioredoxin reductase system (8)]. The functional implications for the majority of the >3,000 SNO proteins identified to date remain obscure.

We have previously reported that LTA4H inhibition prevented vascular remodeling and chronic PHT in bleomycin-exposed neonatal rats (16). In the present study, we observed that rescue $NaNO_2$ significantly decreased lung LTB4 content (product of LTA4H epoxy hydrolase activity) and that rescue therapy with SC57461A partially reversed chronic hypoxic PHT. A potential role for *S*-nitrosylation in modulation of LTA4H activity has not, to our knowledge, been previously described. In addition to production of LTB4, which is known to stimulate inflammation, production of matrix proteins, and to increase smooth muscle contractility and airway/vascular remodeling in the lung (43, 48), LTA4H is also known to act as an aminopeptidase, products of which may also contribute to

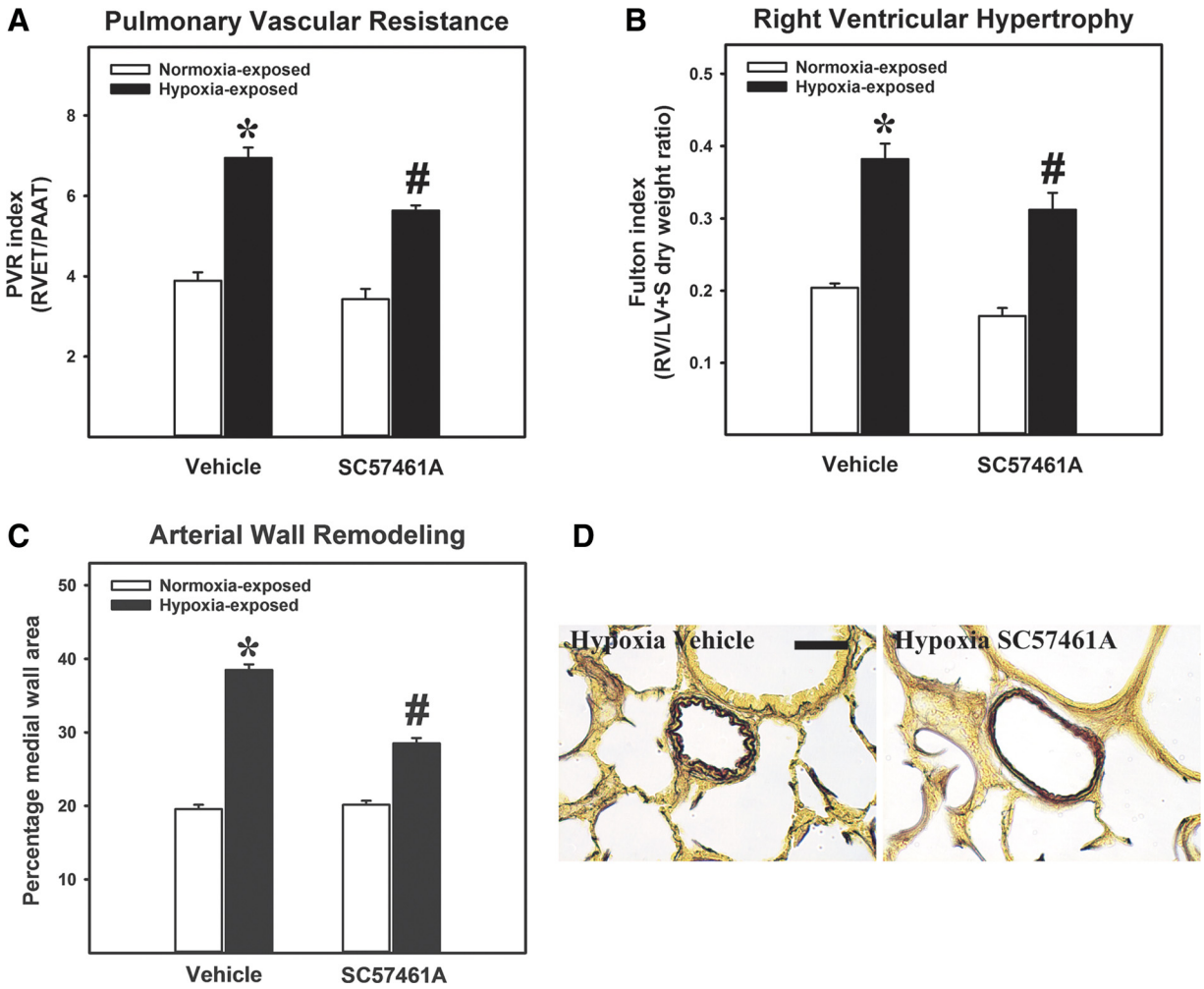

Fig. 5. Rescue treatment with SC57461A, a leukotrieneA4 hydrolase (LTA4H) inhibitor, partially reversed chronic hypoxic pulmonary hypertension (PHT). From *postnatal days 1–21*, rat pups were exposed to normobaric hypoxia (13% O_2) or normoxia (21% O_2). From *days 14–21*, pups received daily subcutaneous injections of SC57461A 10 mg/kg or 20% DMSO in PBS (vehicle). *A* :pulmonary vascular resistance (PVR) index. Ratio of right ventricular ejection time (RVET) to pulmonary arterial acceleration time (PAAT), $n = 8$ animals per group. *B*: right ventricular hypertrophy (RVH) assessed by right ventricle (RV)/left ventricle (LV) + septum (S) weight ratio (Fulton index), $n = 8$ animals per group. *C*: arterial medial wall area as a marker of vascular remodeling, $n = 6$ animals per group. Bars represent means ± SE; $*P < 0.05$, by ANOVA, vs. all other groups. $\#P < 0.05$, by ANOVA, vs. normoxia groups. *D*: high-power photomicrographs demonstrating elastin-stained pulmonary arteries. Bar length = 50 μm.

lung inflammation and injury separate from the leukotriene pathway (40). Our present data provide indirect evidence for inhibitory effects of *S*-nitrosylation on LTA4H activity. The identity of specific cysteine residues on LTA4H that are prone to *S*-nitrosylation and whether inhibition of hydrolase or aminopeptidase pathways predominated in reversal of chronic PHT awaits further study.

Cofilin is an intracellular actin-modulating protein that binds and depolymerizes filamentous F-actin. Cofilin activity is increased in hypertrophic cardiomyocytes (29) and in chronic hypoxia-exposed murine lung (53) and is activated downstream of upregulated RhoA and Rho-kinase activity [via enhanced LIM kinase-mediated phosphorylation (45)]. Pathological Rho-kinase activity is a critical mediator of chronic neonatal PHT in the present model (37, 55, 60), in bleomycin-exposed neonatal rats (34, 37) and in pulmonary hypertensive fetal sheep (21, 22). *S*-nitrosylation is known to modulate the activity of cofilin-1 in endothelial cells (57). In the present study, we observed that lung SNO-cofilin-1 was decreased by chronic exposure to hypoxia and restored by rescue $NaNO_2$. As most SNO protein modifications lead to inhibition of protein function, we speculate that smooth muscle cofilin-1 activity was reduced by enhanced *S*-nitrosylation, potentially also contributing to reversal of vascular remodeling.

There are several limitations to this study. First, it is likely that multiple SNO protein modifications contributed to $NaNO_2$-mediated reversal of chronic PHT; however, we chose to explore LTA4H as a candidate because of amenability to pharmacological inhibition and the known effects of the leukotriene pathway in mediating PHT (16). Of the other candidate SNO proteins identified, all may contribute to the pathogenesis of chronic PHT (modulators of actin depolymerization, oxidative stress, cell survival) and warrant further exploration. Second, although we were able to measure total and specific lung SNOs in whole tissue, we were unable to localize them in situ. Commercially available SNO-nitrosocysteine antibodies are available; however, we were unable to obtain any meaningful data employing several of these antibodies. Third, we

did not explore the relative contributions of NO-cGMP versus SNO signaling in the therapeutic effects of $NaNO_2$. This could be explored in future studies employing a smooth-muscle-specific soluble guanylate cyclase knockout model, either in vitro or in vivo. Finally, although pulmonary-selective (inhalation) therapy with $NaNO_2$ has the greater translational potential, we chose to limit the present study to systemic therapy as proof of concept of efficacy and superiority to iNO.

In conclusion, we provide the first preclinical evidence, to our knowledge, for efficacy of $NaNO_2$ in the immature animal. Ongoing and future studies will examine the utility of the inhalational route of therapy and efficacy in alternative neonatal models that replicate bronchopulmonary dysplasia and other developmental lung disorders.

ACKNOWLEDGMENTS

We thank Dr. Jonathan Krieger (SPARC BioCentre, Hospital for Sick Children, Toronto, Canada) for valuable assistance with multiplex liquid chromatography/TMT spectrometry *S*-nitrosothiol protein measurement and analysis.

GRANTS

This work was supported by operating funding from the Physicians' Services Incorporated Foundation and the Heart and Stroke Foundation of Canada and by infrastructure funding from the Canada Foundation for Innovation (all to R. Jankov).

DISCLOSURES

No conflicts of interest, financial or otherwise, are declared by the authors.

AUTHOR CONTRIBUTIONS

R.P.J. conceived and designed research; R.P.J., K.L.D., S.I., C.K., J.I., N.B.F., and A.J. performed experiments; R.P.J., K.L.D., S.I., N.B.F., and A.J. analyzed data; R.P.J. and A.J. interpreted results of experiments; R.P.J. prepared figures; R.P.J. and A.J. drafted manuscript; R.P.J., K.L.D., C.K., J.I., N.B.F., and A.J. edited and revised manuscript; R.P.J., K.L.D., S.I., C.K., J.I., N.B.F., and A.J. approved final version of manuscript.

REFERENCES

1. **Angelo M, Singel DJ, Stamler JS.** An S-nitrosothiol (SNO) synthase function of hemoglobin that utilizes nitrite as a substrate. *Proc Natl Acad Sci USA* 103: 8366–8371, 2006. doi:10.1073/pnas.0600942103.
2. **Arnelle DR, Stamler JS.** NO+, NO, and NO- donation by S-nitrosothiols: implications for regulation of physiological functions by S-nitrosylation and acceleration of disulfide formation. *Arch Biochem Biophys* 318: 279–285, 1995. doi:10.1006/abbi.1995.1231.
3. **Auten RL, Mason SN, Whorton MH, Lampe WR, Foster WM, Goldberg RN, Li B, Stamler JS, Auten KM.** Inhaled ethyl nitrite prevents hyperoxia-impaired postnatal alveolar development in newborn rats. *Am J Respir Crit Care Med* 176: 291–299, 2007. doi:10.1164/rccm.200605-662OC.
4. **Baliga RS, Milsom AB, Ghosh SM, Trinder SL, Macallister RJ, Ahluwalia A, Hobbs AJ.** Dietary nitrate ameliorates pulmonary hypertension: cytoprotective role for endothelial nitric oxide synthase and xanthine oxidoreductase. *Circulation* 125: 2922–2932, 2012. doi:10.1161/CIRCULATIONAHA.112.100586.
5. **Banks BA, Seri I, Ischiropoulos H, Merrill J, Rychik J, Ballard RA.** Changes in oxygenation with inhaled nitric oxide in severe bronchopulmonary dysplasia. *Pediatrics* 103: 610–618, 1999. doi:10.1542/peds.103.3.610.
6. **Belcastro R, Lopez L, Li J, Masood A, Tanswell AK.** Chronic lung injury in the neonatal rat: up-regulation of TGFβ1 and nitration of IGF-R1 by peroxynitrite as likely contributors to impaired alveologenesis. *Free Radic Biol Med* 80: 1–11, 2015. doi:10.1016/j.freeradbiomed.2014.12.011.
7. **Belik J, Stevens D, Pan J, McIntyre BA, Kantores C, Ivanovska J, Xu EZ, Ibrahim C, Panama BK, Backx PH, McNamara PJ, Jankov RP.** Pulmonary vascular and cardiac effects of peroxynitrite decomposition in newborn rats. *Free Radic Biol Med* 49: 1306–1314, 2010. doi:10.1016/j.freeradbiomed.2010.07.021.
8. **Benhar M, Forrester MT, Stamler JS.** Protein denitrosylation: enzymatic mechanisms and cellular functions. *Nat Rev Mol Cell Biol* 10: 721–732, 2009. doi:10.1038/nrm2764.
9. **Bryan NS, Fernandez BO, Bauer SM, Garcia-Saura MF, Milsom AB, Rassaf T, Maloney RE, Bharti A, Rodriguez J, Feelisch M.** Nitrite is a signaling molecule and regulator of gene expression in mammalian tissues. *Nat Chem Biol* 1: 290–297, 2005. doi:10.1038/nchembio734.
10. **Dalsgaard T, Simonsen U, Fago A.** Nitrite-dependent vasodilation is facilitated by hypoxia and is independent of known NO-generating nitrite reductase activities. *Am J Physiol Heart Circ Physiol* 292: H3072–H3078, 2007. doi:10.1152/ajpheart.01298.2006.
11. **Day RW, Lynch JM, White KS, Ward RM.** Acute response to inhaled nitric oxide in newborns with respiratory failure and pulmonary hypertension. *Pediatrics* 98: 698–705, 1996.
12. **Deruelle P, Balasubramaniam V, Kunig AM, Seedorf GJ, Markham NE, Abman SH.** BAY 41-2272, a direct activator of soluble guanylate cyclase, reduces right ventricular hypertrophy and prevents pulmonary vascular remodeling during chronic hypoxia in neonatal rats. *Biol Neonate* 90: 135–144, 2006. doi:10.1159/000092518.
13. **Deruelle P, Grover TR, Storme L, Abman SH.** Effects of BAY 41-2272, a soluble guanylate cyclase activator, on pulmonary vascular reactivity in the ovine fetus. *Am J Physiol Lung Cell Mol Physiol* 288: L727–L733, 2005. doi:10.1152/ajplung.00409.2004.
14. **Dezfulian C, Raat N, Shiva S, Gladwin MT.** Role of the anion nitrite in ischemia-reperfusion cytoprotection and therapeutics. *Cardiovasc Res* 75: 327–338, 2007. doi:10.1016/j.cardiores.2007.05.001.
15. **Dunlop K, Gosal K, Kantores C, Ivanovska J, Dhaliwal R, Desjardins JF, Connelly KA, Jain A, McNamara PJ, Jankov RP.** Therapeutic hypercapnia prevents inhaled nitric oxide-induced right-ventricular systolic dysfunction in juvenile rats. *Free Radic Biol Med* 69: 35–49, 2014. doi:10.1016/j.freeradbiomed.2014.01.008.
16. **Ee MT, Kantores C, Ivanovska J, Wong MJ, Jain A, Jankov RP.** Leukotriene B4 mediates macrophage influx and pulmonary hypertension in bleomycin-induced chronic neonatal lung injury. *Am J Physiol Lung Cell Mol Physiol* 311: L292–L302, 2016. doi:10.1152/ajplung.00120.2016.
17. **Egemnazarov B, Schermuly RT, Dahal BK, Elliott GT, Hoglen NC, Surber MW, Weissmann N, Grimminger F, Seeger W, Ghofrani HA.** Nebulization of the acidified sodium nitrite formulation attenuates acute hypoxic pulmonary vasoconstriction. *Respir Res* 11: 81, 2010. doi:10.1186/1465-9921-11-81.
18. **Forrester MT, Foster MW, Benhar M, Stamler JS.** Detection of protein S-nitrosylation with the biotin-switch technique. *Free Radic Biol Med* 46: 119–126, 2009. doi:10.1016/j.freeradbiomed.2008.09.034.
19. **Gaston B.** Summary: systemic effects of inhaled nitric oxide. *Proc Am Thorac Soc* 3: 170–172, 2006. doi:10.1513/pats.200506-049BG.
20. **Gaston B, Singel D, Doctor A, Stamler JS.** S-nitrosothiol signaling in respiratory biology. *Am J Respir Crit Care Med* 173: 1186–1193, 2006. doi:10.1164/rccm.200510-1584PP.
21. **Gien J, Seedorf GJ, Balasubramaniam V, Tseng N, Markham N, Abman SH.** Chronic intrauterine pulmonary hypertension increases endothelial cell Rho kinase activity and impairs angiogenesis in vitro. *Am J Physiol Lung Cell Mol Physiol* 295: L680–L687, 2008. doi:10.1152/ajplung.00516.2007.
22. **Gien J, Tseng N, Seedorf G, Roe G, Abman SH.** Endothelin-1 impairs angiogenesis in vitro through Rho-kinase activation after chronic intrauterine pulmonary hypertension in fetal sheep. *Pediatr Res* 73: 252–262, 2013. doi:10.1038/pr.2012.177.
23. **Gole MD, Souza JM, Choi I, Hertkorn C, Malcolm S, Foust RF III, Finkel B, Lanken PN, Ischiropoulos H.** Plasma proteins modified by tyrosine nitration in acute respiratory distress syndrome. *Am J Physiol Lung Cell Mol Physiol* 278: L961–L967, 2000. doi:10.1152/ajplung.2000.278.5.L961.
24. **Gow AJ, Farkouh CR, Munson DA, Posencheg MA, Ischiropoulos H.** Biological significance of nitric oxide-mediated protein modifications. *Am J Physiol Lung Cell Mol Physiol* 287: L262–L268, 2004. doi:10.1152/ajplung.00295.2003.
25. **Gracia R, Shepherd G.** Cyanide poisoning and its treatment. *Pharmacotherapy* 24: 1358–1365, 2004. doi:10.1592/phco.24.14.1358.43149.
26. **Grasemann H, Dhaliwal R, Ivanovska J, Kantores C, McNamara PJ, Scott JA, Belik J, Jankov RP.** Arginase inhibition prevents bleomycin-induced pulmonary hypertension, vascular remodeling, and collagen deposition in neonatal rat lungs. *Am J Physiol Lung Cell Mol Physiol* 308: L503–L510, 2015. doi:10.1152/ajplung.00328.2014.

27. **Hess DT, Stamler JS.** Regulation by S-nitrosylation of protein post-translational modification. *J Biol Chem* 287: 4411–4418, 2012. doi:10.1074/jbc.R111.285742.
28. **Hunter CJ, Dejam A, Blood AB, Shields H, Kim-Shapiro DB, Machado RF, Tarekegn S, Mulla N, Hopper AO, Schechter AN, Power GG, Gladwin MT.** Inhaled nebulized nitrite is a hypoxia-sensitive NO-dependent selective pulmonary vasodilator. *Nat Med* 10: 1122–1127, 2004. doi:10.1038/nm1109.
29. **Hunter JC, Zeidan A, Javadov S, Kilić A, Rajapurohitam V, Karmazyn M.** Nitric oxide inhibits endothelin-1-induced neonatal cardiomyocyte hypertrophy via a RhoA-ROCK-dependent pathway. *J Mol Cell Cardiol* 47: 810–818, 2009. doi:10.1016/j.yjmcc.2009.09.012.
30. **Ibrahim YI, Ninnis JR, Hopper AO, Deming DD, Zhang AX, Herring JL, Sowers LC, McMahon TJ, Power GG, Blood AB.** Inhaled nitric oxide therapy increases blood nitrite, nitrate, and s-nitrosohemoglobin concentrations in infants with pulmonary hypertension. *J Pediatr* 160: 245–251, 2012. doi:10.1016/j.jpeds.2011.07.040.
31. **Jankov RP, Lewis P, Kantores C, Ivanovska J, Xu EZ, Van Vliet T, Lee AH, Tanswell AK, McNamara PJ.** Peroxynitrite mediates right-ventricular dysfunction in nitric oxide-exposed juvenile rats. *Free Radic Biol Med* 49: 1453–1467, 2010. doi:10.1016/j.freeradbiomed.2010.08.007.
32. **Jankov RP, Tanswell AK.** Chronic neonatal lung injury and care strategies to decrease injury. In: *Fetal Lung Development: Clinical Correlates & Future Technologies*, edited by Jobe A, Whitsett JA, Abman SH. New York: Cambridge University Press, 2016, p. 205–222. doi:10.1017/CBO9781139680349.012.
33. **Jones JA, Ninnis JR, Hopper AO, Ibrahim Y, Merritt TA, Wan KW, Power GG, Blood AB.** Nitrite and nitrate concentrations and metabolism in breast milk, infant formula, and parenteral nutrition. *J Parenter Enteral Nutr* 38: 856–866, 2014. doi:10.1177/0148607113496118.
34. **Lee AH, Dhaliwal R, Kantores C, Ivanovska J, Gosal K, McNamara PJ, Letarte M, Jankov RP.** Rho-kinase inhibitor prevents bleomycin-induced injury in neonatal rats independent of effects on lung inflammation. *Am J Respir Cell Mol Biol* 50: 61–73, 2014. doi:10.1165/rcmb.2013-0131OC.
35. **Masood A, Belcastro R, Li J, Kantores C, Jankov RP, Tanswell AK.** A peroxynitrite decomposition catalyst prevents 60% O_2-mediated rat chronic neonatal lung injury. *Free Radic Biol Med* 49: 1182–1191, 2010. doi:10.1016/j.freeradbiomed.2010.07.001.
36. **McMahon TJ, Doctor A.** Extrapulmonary effects of inhaled nitric oxide: role of reversible S-nitrosylation of erythrocytic hemoglobin. *Proc Am Thorac Soc* 3: 153–160, 2006. doi:10.1513/pats.200507-066BG.
37. **McNamara PJ, Murthy P, Kantores C, Teixeira L, Engelberts D, van Vliet T, Kavanagh BP, Jankov RP.** Acute vasodilator effects of Rho-kinase inhibitors in neonatal rats with pulmonary hypertension unresponsive to nitric oxide. *Am J Physiol Lung Cell Mol Physiol* 294: L205–L213, 2008. doi:10.1152/ajplung.00234.2007.
38. **Moya MP, Gow AJ, Califf RM, Goldberg RN, Stamler JS.** Inhaled ethyl nitrite gas for persistent pulmonary hypertension of the newborn. *Lancet* 360: 141–143, 2002. doi:10.1016/S0140-6736(02)09385-6.
39. **Murray CI, Uhrigshardt H, O'Meally RN, Cole RN, Van Eyk JE.** Identification and quantification of S-nitrosylation by cysteine reactive tandem mass tag switch assay. *Mol Cell Proteomics* 11: M111 013441, 2012. doi:10.1074/mcp.M111.013441.
40. **Paige M, Wang K, Burdick M, Park S, Cha J, Jeffery E, Sherman N, Shim YM.** Role of leukotriene A4 hydrolase aminopeptidase in the pathogenesis of emphysema. *J Immunol* 192: 5059–5068, 2014. doi:10.4049/jimmunol.1400452.
41. **Pankey EA, Badejo AM, Casey DB, Lasker GF, Riehl RA, Murthy SN, Nossaman BD, Kadowitz PJ.** Effect of chronic sodium nitrite therapy on monocrotaline-induced pulmonary hypertension. *Nitric Oxide* 27: 1–8, 2012. doi:10.1016/j.niox.2012.02.004.
42. **Peng G, Ivanovska J, Kantores C, Van Vliet T, Engelberts D, Kavanagh BP, Enomoto M, Belik J, Jain A, McNamara PJ, Jankov RP.** Sustained therapeutic hypercapnia attenuates pulmonary arterial Rho-kinase activity and ameliorates chronic hypoxic pulmonary hypertension in juvenile rats. *Am J Physiol Heart Circ Physiol* 302: H2599–H2611, 2012. doi:10.1152/ajpheart.01180.2011.
43. **Peters-Golden M, Henderson WR JR.** Leukotrienes. *N Engl J Med* 357: 1841–1854, 2007. doi:10.1056/NEJMra071371.
44. **Rix PJ, Vick A, Attkins NJ, Barker GE, Bott AW, Alcorn H JR, Gladwin MT, Shiva S, Bradley S, Hussaini A, Hoye WL, Parsley EL, Masamune H.** Pharmacokinetics, pharmacodynamics, safety, and tolerability of nebulized sodium nitrite (AIR001) following repeat-dose inhalation in healthy subjects. *Clin Pharmacokinet* 54: 261–272, 2015. doi:10.1007/s40262-014-0201-y.
45. **Sumi T, Matsumoto K, Nakamura T.** Specific activation of LIM kinase 2 via phosphorylation of threonine 505 by ROCK, a Rho-dependent protein kinase. *J Biol Chem* 276: 670–676, 2001. doi:10.1074/jbc.M007074200.
46. **Thibeault DW, Truog WE, Ekekezie II.** Acinar arterial changes with chronic lung disease of prematurity in the surfactant era. *Pediatr Pulmonol* 36: 482–489, 2003. doi:10.1002/ppul.10349.
47. **Thomas DD, Miranda KM, Colton CA, Citrin D, Espey MG, Wink DA.** Heme proteins and nitric oxide (NO): the neglected, eloquent chemistry in NO redox signaling and regulation. *Antioxid Redox Signal* 5: 307–317, 2003. doi:10.1089/152308603322110887.
48. **Tian W, Jiang X, Sung YK, Qian J, Yuan K, Nicolls MR.** Leukotrienes in pulmonary arterial hypertension. *Immunol Res* 58: 387–393, 2014. doi:10.1007/s12026-014-8492-5.
49. **Torok JA, Brahmajothi MV, Zhu H, Tinch BT, Auten RL, McMahon TJ.** Transpulmonary flux of S-nitrosothiols and pulmonary vasodilation during nitric oxide inhalation: role of transport. *Am J Respir Cell Mol Biol* 47: 37–43, 2012. doi:10.1165/rcmb.2011-0439OC.
50. **Tourneux P, Markham N, Seedorf G, Balasubramaniam V, Abman SH.** Inhaled nitric oxide improves lung structure and pulmonary hypertension in a model of bleomycin-induced bronchopulmonary dysplasia in neonatal rats. *Am J Physiol Lung Cell Mol Physiol* 297: L1103–L1111, 2009. doi:10.1152/ajplung.00293.2009.
51. **van der Vliet A, Eiserich JP, O'Neill CA, Halliwell B, Cross CE.** Tyrosine modification by reactive nitrogen species: a closer look. *Arch Biochem Biophys* 319: 341–349, 1995. doi:10.1006/abbi.1995.1303.
52. **van Faassen EE, Bahrami S, Feelisch M, Hogg N, Kelm M, Kim-Shapiro DB, Kozlov AV, Li H, Lundberg JO, Mason R, Nohl H, Rassaf T, Samouilov A, Slama-Schwok A, Shiva S, Vanin AF, Weitzberg E, Zweier J, Gladwin MT.** Nitrite as regulator of hypoxic signaling in mammalian physiology. *Med Res Rev* 29: 683–741, 2009. doi:10.1002/med.20151.
53. **Veith C, Schmitt S, Veit F, Dahal BK, Wilhelm J, Klepetko W, Marta G, Seeger W, Schermuly RT, Grimminger F, Ghofrani HA, Fink L, Weissmann N, Kwapiszewska G.** Cofilin, a hypoxia-regulated protein in murine lungs identified by 2DE: role of the cytoskeletal protein cofilin in pulmonary hypertension. *Proteomics* 13: 75–88, 2013. doi:10.1002/pmic.201200206.
54. **Wong MJ, Kantores C, Ivanovska J, Jain A, Jankov RP.** Simvastatin prevents and reverses chronic pulmonary hypertension in newborn rats via pleiotropic inhibition of RhoA signaling. *Am J Physiol Lung Cell Mol Physiol* 311: L985–L999, 2016. doi:10.1152/ajplung.00345.2016.
55. **Xu EZ, Kantores C, Ivanovska J, Engelberts D, Kavanagh BP, McNamara PJ, Jankov RP.** Rescue treatment with a Rho-kinase inhibitor normalizes right ventricular function and reverses remodeling in juvenile rats with chronic pulmonary hypertension. *Am J Physiol Heart Circ Physiol* 299: H1854–H1864, 2010. doi:10.1152/ajpheart.00595.2010.
56. **Yingchoncharoen T, Rakyhao T, Chuncharunee S, Sritara P, Pienvichit P, Paiboonsukwong K, Sathavorasmith P, Sirirat K, Sriwantana T, Srihirun S, Sibmooh N.** Inhaled nebulized sodium nitrite decreases pulmonary artery pressure in beta-thalassemia patients with pulmonary hypertension. *Nitric Oxide* 76: 174–178, 2018. doi:10.1016/j.niox.2017.09.010.
57. **Zhang HH, Lechuga TJ, Tith T, Wang W, Wing DA, Chen DB.** S-nitrosylation of cofilin-1 mediates estradiol-17β-stimulated endothelial cytoskeleton remodeling. *Mol Endocrinol* 29: 434–444, 2015. doi:10.1210/me.2014-1297.
58. **Zhang J, Xin L, Shan B, Chen W, Xie M, Yuen D, Zhang W, Zhang Z, Lajoie GA, Ma B.** PEAKS DB: de novo sequencing assisted database search for sensitive and accurate peptide identification. *Mol Cell Proteomics* 11: M111.010587, 2012. doi:10.1074/mcp.M111.010587.
59. **Zhu S, Kachel DL, Martin WJ II, Matalon S.** Nitrated SP-A does not enhance adherence of Pneumocystis carinii to alveolar macrophages. *Am J Physiol Lung Cell Mol Physiol* 275: L1031–L1039, 1998.
60. **Ziino AJ, Ivanovska J, Belcastro R, Kantores C, Xu EZ, Lau M, McNamara PJ, Tanswell AK, Jankov RP.** Effects of rho-kinase inhibition on pulmonary hypertension, lung growth, and structure in neonatal rats chronically exposed to hypoxia. *Pediatr Res* 67: 177–182, 2010. doi:10.1203/PDR.0b013e3181c6e5a7.
61. **Zuckerbraun BS, George P, Gladwin MT.** Nitrite in pulmonary arterial hypertension: therapeutic avenues in the setting of dysregulated arginine/nitric oxide synthase signalling. *Cardiovasc Res* 89: 542–552, 2011. doi:10.1093/cvr/cvq370.
62. **Zweier JL, Li H, Samouilov A, Liu X.** Mechanisms of nitrite reduction to nitric oxide in the heart and vessel wall. *Nitric Oxide* 22: 83–90, 2010. doi:10.1016/j.niox.2009.12.004.